Synthesis, Structure, and Coordination Chemistry of a Tridentate, Six-Electron-Donor Amidinate Ligand

Kristi Kincaid, Christopher P. Gerlach, Garth R. Giesbrecht, John R. Hagadorn, Glenn D. Whitener, Alex Shafir, and John Arnold*

Department of Chemistry, University of California, Berkeley, and Chemical Sciences Division, Lawrence Berkeley National Laboratory, Berkeley, California 94720-1460

The coordination chemistry of ancillary amidinate ligands with a pendant pyridine functionality is described. Reaction of *p*-toluoyl- or *p*-^{t}Bu-benzoyl chloride with 2-amino-ethylpyridine generates the amides 2-Py-$(CH_2)_2$NHCO(*p*-RPh) (R = Me **1a**; ^{t}Bu **1b**); these amides are then converted to the amidines 2-Py-$(CH_2)_2$NHC(*p*-RPh)NR′ (R = Me, R′ = Ph (**2a**) (L^{Me}H); R = ^{t}Bu, R′ = 3,5-dimethylphenyl (**2b**) (L^{tBu}H)) by reaction with PCl_5 followed by R′NH_2. The amidines **2a,b** were characterized by ^{1}H NMR and IR spectroscopy and elemental analyses, and **2b** was characterized by X-ray crystallography. Reaction of **2a** or **2b** with homoleptic metal−alkyls or −amides yields the mono- or bis(amidinate) complexes $(L^{Me})_2$Mg (**3a**), (L^{tBu})AlMe$_2$ (**4**), (L^{tBu})Zr$(CH_2Ph)_3$ (**5**), and $(L^{Me})_2$La[N(SiMe$_3$)$_2$] (**6**). All metal complexes were characterized by ^{1}H NMR and IR spectroscopy, elemental analyses, and X-ray crystallography. The X-ray crystal structures of compounds **3**−**6** show them to be monomeric, with the pendant pyridine coordinated intramolecularly in all cases. The tridentate amidinate coordinates meridionally to the metal center except in the case of the lanthanum derivative **6**, where an approximate facial geometry is observed.

Introduction

The ability of amidinates [RC(NR′)$_2$]$^-$ to act as four-electron, bidentate ligands for main group elements, transition metals, and the lanthanides is well established.[1,2] Amidinates have proven to be versatile ligands due to the ease with which the steric and electronic properties of the resultant metal complexes can be tuned by means of substitution at the nitrogen atoms. Previous work from our group has expanded the scope of these ligands by linking two amidinates together to produce *C₂* symmetric ligand systems that are loosely analogous to *ansa*-Cp systems.[3,4] Here we report the high-yield synthesis of a series of easily prepared amidines with a pendant pyridine moiety. In this first account, our aim is to demonstrate their versatility to act as ligands toward a variety of metals from across the periodic table. As shown here, compared to simple amidines, the ability of these compounds to act as six-electron-donor, three-coordinate ligands renders them closer analogues to Cp ligands;[5] nonetheless, their tendency to adopt meridional geometries clearly sets them apart from η^5-Cp ligands where only facial coordination is possible. Reactivity studies on these and related compounds will be addressed in forthcoming papers.
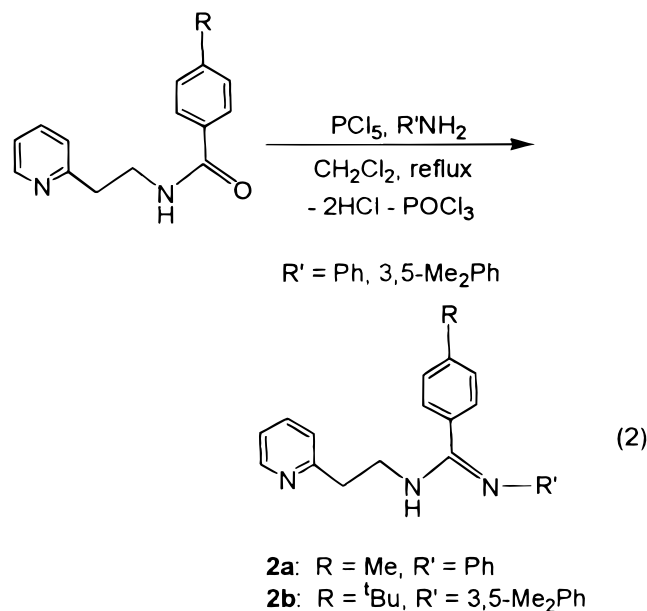
Results and Discussion

Amidine Synthesis. Synthesis of the (2-pyridine)-ethyl-functionalized benzamidinate was accomplished by conversion of a suitable amide to an imine chloride, which was then reacted with a substituted aniline to yield the desired amidine. We employed related methodology previously in the synthesis of linked bis-(amidines),[4] and the route has been used by others to prepare symmetric, bulky amidinates.[6,7] The starting amide was formed in high yield by reaction of *p*-R-benzoyl chloride with 2-aminoethylpyridine in the presence of triethylamine (eq 1).

1a: R = Me
1b: R = ^{t}Bu
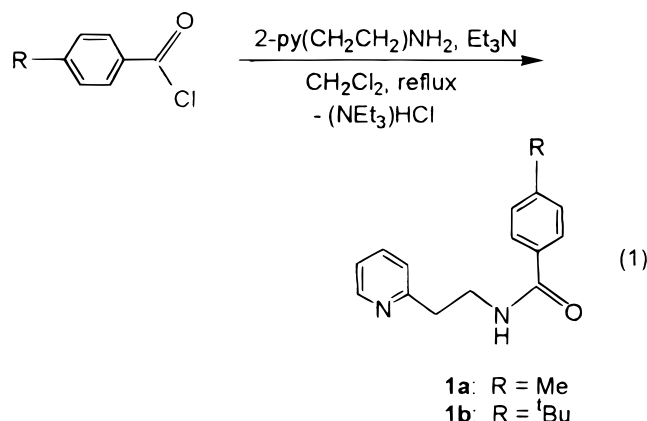
The amides **1a,b** were then converted to the corresponding amidines by in situ generation of imine

(1) Edelmann, F. T. *Coord. Chem. Rev.* **1994**, *137*, 403.
(2) Barker, J.; Kilner, M. *Coord. Chem. Rev.* **1994**, *133*, 219.
(3) Hagadorn, J. R.; Arnold, J. *Angew. Chem., Int. Ed. Engl.* **1998**, *37*, 1729.
(4) Whitener, G. D.; Hagadorn, J. R.; Arnold, J. *J. Chem. Soc., Dalton. Trans.* **1999**, 1249.
(5) During the preparation of this article, the synthesis of an amidinate ligand with a pendant dimethylamino group was described: (a) Brandsma, M. J. R.; Brussee, E. A. C.; Meetsma, A.; Hessen, B.; Teuben, J. H. *Eur. J. Inorg. Chem.* **1998**, 1867. An amidinate ligand with a noncoordinating dimethylamino group has also been reported: (b) Hao, S.; Gambarotta, S.; Bensimon, C.; Edema, J. J. H. *Inorg. Chim. Acta* **1993**, *213*, 65.

(6) Boere, R. T.; Klassen, V.; Wolmershauser, G. *J. Chem. Soc., Dalton Trans.* **1998**, 4147.
(7) Boyd, G. V. In *The Chemistry of Amidines and Imidates*; Patai, S., Rappoport, Z., Eds.; John Wiley & Sons: Chichester, 1991; Vol. 2, pp 339−366.

chlorides via reaction with PCl_5; these species readily reacted with substituted anilines in the presence of triethylamine to generate amidines **2a**,**b** in moderate yields (eq 2).

$$PCl_5, R'NH_2 \qquad CH_2Cl_2, \text{reflux} \qquad -2HCl - POCl_3$$

R' = Ph, 3,5-Me$_2$Ph

(2)

2a: R = Me, R' = Ph
2b: R = ^{t}Bu, R' = 3,5-Me$_2$Ph

The amidines **2a** (L^{Me}H) and **2b** (L^{tBu}H) are soluble in solvents such as ether, benzene, and toluene and were isolated as colorless crystals from diethyl ether solutions. Compared to the unsubstituted analogue, incorporation of *tert*-butyl and *meta*-methyl groups in **2b** was beneficial, as it both increased the solubility of the ligand and provided two convenient ^{1}H NMR handles. The proton occupying the 6-position of the pyridine ring appears as a doublet at ~8.5 ppm in the ^{1}H NMR spectrum. The shift of this signal to lower field is diagnostic of coordination of the pyridine arm to a metal center (see below). Additionally, the methylene protons of the ethylene spacer appear as broad singlets at room temperature in the starting amidines. These signals sharpen on cooling to 0 °C, where the A$_2$B$_2$ system is fully resolved; likewise, coordination of the ligand to a metal center has the same effect. The amidine protons reside at ~5.4 ppm for both **2a** and **2b**, upfield of most common amines[8] but similar to a series of cyclohexyl-linked bis(amidines) reported earlier.[4] IR spectra of the amidines show characteristic NH stretches in the range $3275-3250$ cm^{-1} along with strong absorbances around 1600 cm^{-1} due to $\nu_{C=N}$.

An ORTEP view of the molecular structure of L^{tBu}H (**2b**) is shown in Figure 1; bond lengths and angles are given in Table 1. Complete details of the crystallographic analyses of compounds **2b**–**6** are given in Table 6. The two C−N bonds in the amidine (N2−C8, 1.362-(5) Å) and N3−C8, 1.301(5) Å) are similar in length to those reported for other bulky amidines,[6] indicating the localized nature of the N−C double bond. Consistent with this view, electron density in accord with a single amidine proton (H28) was located on N2. In the solid state, **2b** is monomeric, in contrast to a number of
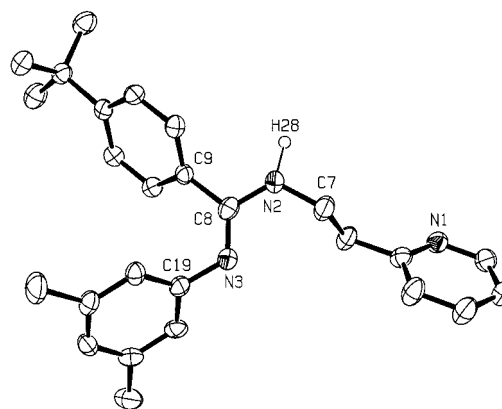
(8) Silverstein, R. M.; Bassler, G. C.; Morrill, T. C. *Spectrometric Identification of Organic Compounds*; John Wiley & Sons: New York, 1991.

Figure 1. ORTEP view of L^{tBu}H (**2b**) drawn with 50% probability ellipsoids.

Table 1. Selected Bond Distances (Å) and Angles (deg) for L^{tBu}H (2b)

N2−C8	1.362(5)	N3−C8	1.301(5)
N2−C7	1.464(5)	N3−C19	1.414(5)
C8−C9	1.494(5)		
N2−C8−N3	120.3(4)	N3−C8−C9	126.7(4)
N2−C8−C9	112.9(4)	C8−N3−C19	120.9(3)
C7−N2−C8	121.8(3)		

Table 2. Selected Bond Distances (Å) and Angles (deg) for (L^{Me})$_2$Mg(THF) (3a)

N2−C8	1.322(5)	N3−C8	1.339(5)
N5−C29	1.321(5)	N6−C29	1.346(5)
Mg1−N1	2.264(4)	Mg1−N2	2.104(4)
Mg1−N3	2.211(4)	Mg1−N4	2.260(4)
Mg1−N5	2.110(4)	Mg1−N6	2.198(4)
N2−C8−N3	113.4(4)	N5−C29−N6	113.5(4)
N1−Mg1−N2	82.8(1)	N1−Mg1−N3	144.7(1)
N2−Mg1−N3	62.0(1)	N4−Mg1−N5	84.0(1)
N4−Mg1−N6	145.3(1)	N5−Mg1−N6	62.3(1)

Table 3. Selected Bond Distances (Å) and Angles (deg) for (L^{tBu})AlMe$_2$ (4)

N2−C8	1.368(8)	N3−C8	1.381(8)
Al1−N1	2.218(6)	Al1−N2	1.898(6)
Al1−N3	2.083(5)	Al1−C27	1.986(8)
Al1−C28	2.030(8)		
N2−C8−N3	117.7(6)	N1−Al1−N2	79.1(2)
N1−Al1−N3	151.4(2)	N1−Al1−C27	88.1(3)
N1−Al1−C28	112.3(2)	N2−Al1−N3	72.3(2)
N2−Al1−C27	119.4(3)	N2−Al1−C28	118.1(3)
N3−Al1−C27	106.9(3)	N3−Al1−C28	81.0(3)
C27−Al1−C28	121.5(3)		

Table 4. Selected Bond Distances (Å) and Angles (deg) for (L^{tBu})Zr(CH$_2$Ph)$_3$ (5)

N2−C8	1.34(1)	N3−C8	1.328(1)
Zr1−N1	2.393(6)	Zr1−N2	2.169(6)
Zr1−N3	2.248(6)	Zr1−C27	2.347(8)
Zr1−C34	2.364(8)	Zr1−C41	2.331(8)
N2−C8−N3	109.7(6)	N1−Zr1−N2	78.4(2)
N1−Zr1−N3	137.5(2)	N2−Zr1−N3	59.2(2)
N1−Zr1−C27	77.3(2)	N1−Zr1−C34	139.2(2)
N1−Zr1−C41	78.6(2)	N2−Zr1−C27	102.8(2)
N2−Zr1−C34	142.4(3)	N2−Zr1−C41	101.7(3)
N3−Zr1−C27	112.5(3)	N3−Zr1−C34	83.1(2)
N3−Zr1−C41	105.9(3)	C27−Zr1−C34	91.3(3)
C27−Zr1−C41	141.1(3)	C34−Zr1−C41	87.2(3)
Zr1−C27−C28	107.4(5)	Zr1−C34−C35	104.0(5)
Zr1−C41−C42	111.5(5)		

amidines that form dimers via intermolecular hydrogen bonds.[6,9]

Table 5. Selected Bond Distances (Å) and Angles (deg) for $(L^{Me})_2La[N(SiMe_3)_2]$ (6)

N2–C8	1.319(6)	N3–C8	1.338(6)
N5–C29	1.319(6)	N6–C29	1.347(6)
La1–N1	2.753(4)	La1–N2	2.491(4)
La1–N3	2.609(4)	La1–N4	2.747(4)
La1–N5	2.599(4)	La1–N6	2.598(4)
La1–N7	2.453(4)		
N2–C8–N3	114.6(4)	N5–C29–N6	113.8(4)
N1–La1–N2	70.4(1)	N1–La1–N3	111.4(1)
N2–La1–N3	52.0(1)	N4–La1–N5	69.6(1)
N4–La1–N6	91.0(1)	N5–La1–N6	50.9(1)
N7–La1–N1	98.3(1)	N7–La1–N2	95.2(1)
N7–La1–N3	118.7(1)	N7–La1–N4	87.4(1)
N7–La1–N5	108.2(1)	N7–La1–N6	157.7(1)

Synthesis of Metal Complexes. Syntheses of mono- and bis-ligand metal complexes were easily accomplished by alkyl or amine elimination reactions between amidines **2a,b** and a range of homoleptic metal alkyl or amide compounds, as shown in eq 3.

$$xL^R H + MR'_y \xrightarrow{\text{ether or THF}} (L^R)_x MR'_{y-x} + xR'H \quad (3)$$
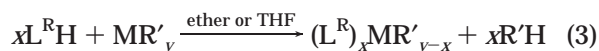
3a: M = Mg, R = Me, R' = Bu, $x = 2$, $y = 2$.
  3b: M = Mg, R = ^{t}Bu, R' = Bu, $x = 2$, $y = 2$.
   4: M = Al, R = ^{t}Bu, R' = Me, $x = 1$, $y = 3$.
   5: M = Zr, R = ^{t}Bu, R' = CH$_2$Ph, $x = 1$, $y = 4$.
   6: M = La, R = Me, R' = N(SiMe$_3$)$_2$, $x = 2$, $y = 3$.

The metal derivatives **3**–**6** were conveniently prepared in high yield as colorless or yellow crystalline powders. The relatively low yield of the lanthanum derivative **6** (42% as compared to 75–91% for **3**–**5**) is a reflection of redistribution chemistry to produce the tri- and mono-substituted products as identified by ^{1}H NMR spectroscopy.

Proton NMR data are useful indicators of complex formation. For example, the amidine proton is absent in spectra of **3**–**6**, and a downfield NMR shift of the *ortho* pyridine proton is a clear marker of coordination of the pendant donor arm to the metal, residing at progressively lower field with increasing metal size (see Experimental Section). The broad methylene resonances of the ethylene spacer found in amidines **2a,b** are also noticeably sharper in metal complexes **3**–**6**, an effect that appears to be diagnostic of coordination of the pyridine. IR spectra of the metal derivatives exhibit C=N stretches only slightly shifted from the starting amidines at ~1600 cm^{-1}.

All of the metal derivatives were characterized by X-ray crystallography, which shows them to be monomeric species in the solid state. The magnesium complex $(L^{Me})_2$Mg crystallized on cooling a saturated THF solution of **3a** to −30 °C overnight. The structure is shown in Figure 2, with a list of relevant bond lengths and angles available in Table 2. Despite the strong tendency of magnesium amidines to coordinate donor solvents such as THF[10] or PhCN,[11] the unit cell contains only a

single molecule of unbound THF. The ligands are coordinated meridionally, with the amidinate nitrogens and the magnesium center defining two planes at a right angle to each other (85.61°). The deviation from planarity within the two planes is 0.0276 Å (amidinate containing N1, N2, and N3) and 0.0806 Å (amidinate containing N4, N5, and N6). The amidinate nitrogen bond lengths in **3a** (2.104(4)−2.211(4) Å) are similar to those reported for [^{i}PrNC(Ph)N^{i}Pr]$_2$Mg(THF)$_2$ (2.164 Å (av))[10] and [Me$_3$SiNC(Ph)NSiMe$_3$]$_2$Mg(PhCN) (2.125 Å (av))[11] and are slightly shorter than the pyridine−magnesium bonds (2.260(4) and 2.264(4) Å).

Yellow crystals of the aluminum derivative were obtained by layering a saturated CH$_2$Cl$_2$ solution of **4** with THF. An ORTEP view of the molecular structure is given in Figure 3; selected bond lengths and angles are presented in Table 3. The structure confirms that the compound is monomeric with a single amidine ligand coordinated to the aluminum center in a meridional fashion. The geometry is distorted trigonal bipyramidal, with N1 and N3 occupying the axial positions (N1−Al1−N3 151.4(2)°). The N2, C27, and C28 atoms reside equatorially, forming angles subtended by aluminum of ~120°. The N2−Al1−N3 bite angle (72.3(2)°) is somewhat larger than those reported for a series of mono-amidinate dimethylaluminum compounds by Jordan et al. (68.2−69.1°).[12,13] The C27−Al1−C28 angle of 121.5(3)° is also slightly larger than those cited in the above series (114.2−118.6°). The N2−C8 and N3−C8 bond lengths are similar (1.368(8) and 1.381(8) Å, respectively), consistent with delocalization within the amidine functionality. The amidinate nitrogen−aluminum bonds (N2−Al1 = 1.898(6) Å, N3−Al1 2.083(5) Å) are shorter than the pyridine nitrogen−aluminum bond (N1−Al1 2.218(6) Å), but comparable to those of other similar dialkyl species (~1.93 Å).[12,14] The Al−Me bonds are longer (C27−Al1 1.986(8) Å, C28−Al1 2.030(8) Å) than in other mono-amidinate species (~1.96 Å)[12,13] as a result of the higher coordination number. (For comparison, the terminal Al−Me bond distance in Al$_2$Me$_6$ is 1.97 Å.[15])

Crystals of (L^{tBu})Zr(CH$_2$Ph)$_3$ (**5**) were grown by cooling a saturated ether solution to −30 °C. An ORTEP representation is shown in Figure 4; a partial list of bond lengths and angles is given in Table 4. The amidinate ligand is coordinated meridionally, with a mirror plane roughly defined by the Zr1, N1, N2, N3, and C34 atoms (deviation 0.0204 Å). The six-coordinate metal is strongly distorted from octahedral, with the axial C27−Zr1−C41 angle of only 141.1(3)°, and, overall, the geometry is perhaps better described as approaching trigonal prismatic. Despite the low electron count—the complex is formally 12 electrons—there is no evidence for agostic interactions, as the Zr−C−C angles are all close to tetrahedral (104.0(5)−111.5(5)°). For comparison, the isoelectronic complex CpZr(CH$_2$Ph)$_3$ is considered to show Zr−C−C angles substantially less than tetrahedral due to the presence of agostic C−H- - -Zr

(9) Hafelinger, G.; Kuske, K. H. In *The Chemistry of Amidines and Imidates*; Patai, S., Rappoprt, Z., Eds.; John Wiley & Sons: Chichester, 1991; Vol. 2, pp 1−100.
(10) Srinivas, B.; Chang, C. C.; Chen, C. H.; Chiang, M. Y.; Chen, I. T.; Wang, Y.; Lee, G. H. *J. Chem. Soc., Dalton Trans.* **1997**, 957.
(11) Westerhausen, M.; Hausen, H. D. *Z. Anorg. Allg. Chem.* **1992**, *615*, 27.

(12) Coles, M. P.; Swenson, D. C.; Jordan, R. F.; Young, V. G. *Organometallics* **1997**, *16*, 5183.
(13) Coles, M. P.; Swenson, D. C.; Jordan, R. F.; Young, V. G. *Organometallics* **1998**, *17*, 4042.
(14) Lechler, R.; Hausen, H. D.; Weidlin, J. *J. Organomet. Chem.* **1989**, *359*, 1.
(15) Vranka, R. G.; Amma, E. L. *J. Am. Chem. Soc.* **1967**, *89*, 3121.

Table 6. Crystallographic Data

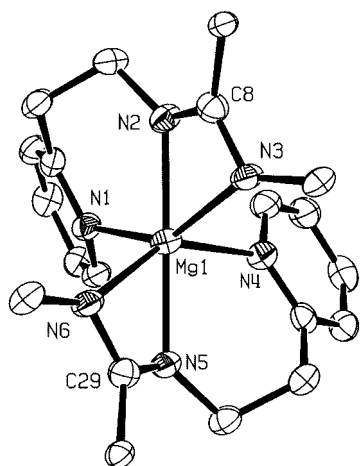|	2b	3a(THF)	4	5	6
formula	$C_{26}H_{31}N_3$	$C_{46}H_{48}N_6OMg$	$C_{28}H_{36}N_3Al$	$C_{47}H_{51}N_3Zr$	$C_{48}H_{58}N_7Si_2La$
fw	385.55	725.23	441.59	749.16	928.11
color, habit	yellow, needle	yellow, block	yellow, plate	yellow, needle	yellow, needle
crystal size, mm	$0.30 \times 0.16 \times 0.15$	$0.24 \times 0.20 \times 0.05$	$0.20 \times 0.18 \times 0.05$	$0.22 \times 0.15 \times 0.08$	$0.25 \times 0.10 \times 0.08$
crystal system	orthorhombic	triclinic	monoclinic	triclinic	monoclinic
space group	*Pnna*	*P*$\bar{1}$	*P*$2_1/c$	*P*$\bar{1}$	*C2/c*
a, Å	22.122(1)	11.7242(7)	16.6814(9)	9.9506(10)	37.2885(24)
b, Å	17.516(1)	12.3840(7)	8.3560(5)	11.0008(2)	10.8058(7)
c, Å	11.581(1)	15.3909(9)	19.0415(11)	19.7062(4)	23.5483(13)
α, deg	90	101.034(1)	90	89.975(1)	90
β, deg	90	107.310(1)	106.224(2)	80.585(1)	95.958(1)
γ, deg	90	96.377(1)	90	65.909(1)	90
V, Å^3	4487(1)	2060(3)	2548(2)	1937(2)	9437(4)
Z	8	2	4	2	8
D_c, g/cm^3	1.14	1.17	1.15	1.28	1.31
$2\theta_{max}$	46.5	52.0	59.1	52.2	52.3
T, °C	-105	-128	-105	-104	-102
total no. of reflns	18960	9838	12396	9272	22946
no. of indep reflns	3639	6874	4875	6479	8833
T_{max}	0.969	1.000	1.000	0.977	0.942
T_{min}	0.827	0.752	0.830	0.743	0.757
μ(Mo Kα), cm^{-1}	0.67	0.85	0.99	3.20	9.92
R_{int}	0.08	0.03	0.09	0.04	0.06
R	0.040	0.063	0.061	0.062	0.031
R_w	0.044	0.068	0.063	0.079	0.032
GOF	1.24	1.73	1.66	2.39	0.95
no. of data	1526	3769	1692	5042	4345

Figure 2. ORTEP view of (L^{Me})$_2$Mg(THF) (**3a**) drawn with 50% probability ellipsoids. Only the *ipso* carbons of the *p*-tolyl and phenyl groups are shown for clarity. One cocrystallized molecule of THF is also omitted.

Figure 3. ORTEP view of (L^{tBu})AlMe$_2$ (**4**) drawn with 50% probability ellipsoids.

interactions.[16] Conversely, the bis(amidinate) species [Me$_3$SiNC(Ph)NSiMe$_3$]$_2$Zr(CH$_2$Ph)$_2$ features larger Zr–C–C angles of 117.6(2)° and 116.6(2)°.[17] The N2–C8 and N3–C8 bond lengths are identical, again implying a delocalized double bond. Complex **5** exhibits two short (2.169(6) and 2.248(6) Å) and one longer (2.393(6) Å) Zr–N bond, a common feature of all the metal complexes presented here. These compare with bond lengths of 2.278 (av) and 2.259 Å (av) in related zirconium amidinates [Me$_3$SiNC(Ph)NSiMe$_3$]$_2$ZrMe$_2$[17,18] and [Me$_3$-SiNC(Ph)NSiMe$_3$]$_2$Zr(CH$_2$Ph)$_2$,[17] respectively. The Zr–C bond lengths are similar to those reported for CpZr(CH$_2$-Ph)$_3$[16] and [Me$_3$SiNC(Ph)NSiMe$_3$]$_2$Zr(CH$_2$Ph)$_2$[17] and are otherwise unremarkable.

Yellow crystals of (L^{Me})$_2$La[N(SiMe$_3$)$_2$] (**6**) were obtained by layering a saturated ether solution with hexanes. The molecular structure of **6** is presented is Figure 5 along with a partial list of bond lengths and angles (Table 5). The large lanthanum center is able to support two three-coordinate substituted-benzamidinates as well as a bulky N(SiMe$_3$)$_2$$^-$ group. In contrast to the metal complexes previously described, in **6** the coordination of the ancillary ligands to the metal center is intermediate between meridional and facial. This is due to the increased steric congestion around the metal because of the bulky amido ligand, which does not allow for the presence of two meridional amidinate ligands as in the magnesium derivative, **3a**. The ligand containing N1, N2, and N3 coordinates with a geometry close to meridional; the sum of the three N–La–N angles is 233.8°. For the other amidine, this sum drops to 211.5° as the ligand approaches a facial geometry. As expected, the amidinate nitrogen–lanthanum bonds (2.491(4)–2.609(4) Å) are substantially shorter than the pyridine nitrogen–lanthanum bonds (2.747(4) and 2.753(4) Å). Although numerous lanthanide amidinate species are

(16) Scholz, J.; Rehbaum, F.; Thiele, K. H.; Goddard, R.; Betz, P.; Kruger, C. *J. Organomet. Chem.* **1993**, *443*, 93.
(17) Walther, D.; Fischer, R.; Gorls, H.; Koch, J.; Schweder, B. *J. Organomet. Chem.* **1996**, *508*, 13.
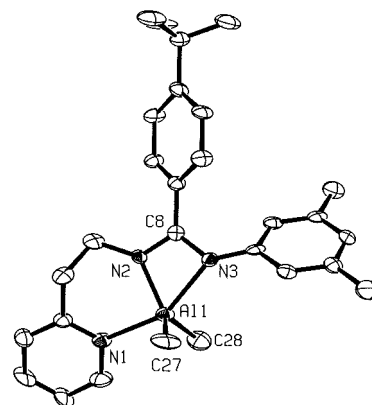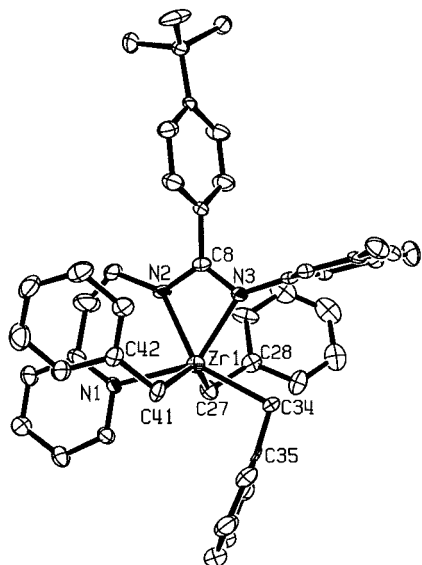
Figure 4. ORTEP view of (L^{tBu})Zr(CH$_2$Ph)$_3$ (**5**) drawn with 50% probability ellipsoids.
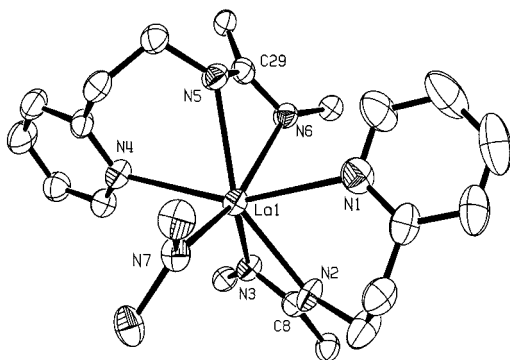

Figure 5. ORTEP view of (L^{Me})$_2$La[N(SiMe$_3$)$_2$] (**6**) drawn with 50% probability ellipsoids. Only the *ipso* carbons of the *p*-tolyl and phenyl groups are shown for clarity. Silyl methyl groups of the amide have also been removed.

known, there are no lanthanum derivatives for comparison, nor has the corresponding pentamethylcyclopentadienyl complex, Cp*$_2$La[N(SiMe$_3$)$_2$],[19] been characterized crystallographically. Nonetheless, the lanthanum–bis(trimethylsilyl)amide bond length of 2.453(4) Å may be compared to a La–N distance of 2.323(10) Å in Cp*$_2$LaNHCH$_3$(NH$_2$CH$_3$)[19] and those in {La[N(SiMe$_3$)$_2$]$_3$}(PPh$_3$O), which range from 2.38(2) to 2.41(2) Å.[20]

Summary and Conclusions

The synthesis of an amidine ligand with a pendant pyridine functionality was easily accomplished by utilizing known synthetic procedures for the generation of amidines. The synthetic route employed here is attractive in that the intermediate amide and the resulting amidine can both be produced in relatively high yield in multigram quantities. Additionally, the amidines are easily functionalized to either increase the solubility of

(18) Hagadorn, J. R.; Arnold, J. *J. Chem. Soc., Dalton Trans.* **1997**, 3087.
(19) Gagne, M. R.; Stern, C. L.; Marks, T. J. *J. Am. Chem. Soc.* **1992**, *114*, 275.
(20) Bradley, D. C.; Ghotra, J. S.; Hart, F. A.; Hursthouse, M. B.; Raithby, P. R. *J. Chem. Soc., Dalton Trans.* **1977**, 1166.

the metal complexes or to provide additional NMR handles within the ligand framework.

Overall, the pyridine-substituted amidine described here appears to be a versatile ligand, forming a wide range of metal mono- and bis-ligand derivatives via alkyl or amine elimination reactions. The choice of amidine (**2a** or **b**) allows for a range of solubility and/or crystallinity of the final product: for example, whereas both ligand systems yielded highly crystalline magnesium salts (**3a** or **b**), the *p*-tolyl-substituted amidine had to be employed in order to isolate a crystalline lanthanum derivative. The amidine ligand appears to prefer meridional coordination as evidenced by the structures of the Mg, Zr, and Al derivatives; however, as seen in the crystal structure of the lanthanum species, (L^{Me})$_2$-La[N(SiMe$_3$)$_2$] (**6**), when the metal center is sufficiently crowded, the ligand can adopt a more facial geometry. The reaction chemistry of the metal complexes described here is the subject of ongoing work.

Experimental Section

General Considerations. Standard Schlenk-line and glovebox techniques were used unless stated otherwise.[21] Diethyl ether, hexanes, dichloromethane, and tetrahydrofuran were purified by passage through a column of activated alumina and degassed with argon.[22] C$_6$D$_6$ and CDCl$_3$ were vacuum transferred from sodium/benzophenone and CaH$_2$, respectively. *p*-Toluoyl chloride, *p*-^{t}Bu-benzoyl chloride, PCl$_5$, Bu$_2$-Mg, and AlMe$_3$ were purchased from Aldrich and used as received. Triethylamine was purchased from Aldrich and distilled from Na. Aniline and 3,5-dimethylaniline were purchased from Aldrich and distilled from CaH$_2$. 2-Aminoethylpyridine,[23] Zr(CH$_2$Ph)$_4$,[24,25] and La[N(SiMe$_3$)$_2$]$_3$[26] were prepared according to literature procedures. Melting points were determined in sealed capillary tubes under nitrogen and are uncorrected. ^{1}H NMR spectra were recorded at ambient temperature unless otherwise stated; chemical shifts are given relative to C$_6$D$_5$H (7.15 ppm) or CHCl$_3$ (7.24 ppm). IR samples were prepared as Nujol mulls and taken between KBr plates. Elemental analyses and mass spectral data were determined at the College of Chemistry, University of California, Berkeley. In some cases, we routinely experienced carbon analyses that gave lower than expected values (ca. 1–2%). In these cases, samples from different preparations were analyzed and more forcing conditions were employed in the analyzer (longer combustion times, addition of catalyst). Without exception, the data were reproducible, and thus we suspect that formation of refractory carbides is responsible. Single-crystal X-ray structure determinations were performed at CHEXRAY, University of California, Berkeley.

2-Py-(CH$_2$)$_2$NHCO(*p*-RPh) (R = Me (1a); ^{t}Bu (1b)). This reaction was performed without the exclusion of air. For **1b**: To a solution of *p*-^{t}Bu-benzoyl chloride (24.7 mL, 126 mmol) and triethylamine (19.3 mL, 139 mmol) in dichloromethane at 0 °C was slowly added 2-aminoethylpyridine (15.0 mL, 126 mmol) via syringe, generating a yellow precipitate. The mixture was allowed to warm to room temperature and then brought to reflux overnight. The dark yellow solution was cooled to room temperature and the solvent removed under vacuum. After trituration with water, the yellow solid was washed with hexanes (2 × 50 mL) and vacuum-dried overnight to yield a white solid (30.8 g, 86%). **1a** was prepared in a similar fashion. (96%). **1a:** Mp: 110–112 °C. ^{1}H NMR (CDCl$_3$, 300 MHz): δ 8.55 (d, 1H, *6-pyH*, $^3J_{H-H}$ = 6.6 Hz), 7.68 (m,

(21) Shriver, E. F.; Bredzon, M. A. *The Manipulation of Air-Sensitive Compounds*; John Wiley & Sons: New York, 1986.
(22) Pangborn, A. B.; Giardello, M. A.; Grubbs, R. H.; Rosen, R. K.; Timmers, F. J. *Organometallics* **1996**, *15*, 1518.
(23) Magnus, G.; Levine, R. *J. Am. Chem. Soc.* **1956**, *78*, 4127.

1H), 7.65 (m, 1H), 7.61 (t, 1H, $^3J_{H-H}$ = 4.8 Hz), 7.49 (br s, 1H, N*H*), 7.21−7.13 (m, 4H), 3.84 (q, 2H, C*H*$_2$, $^3J_{H-H}$ = 5.4 Hz), 3.08 (t, 2H, C*H*$_2$, $^3J_{H-H}$ = 5.4 Hz), 2.37 (s, 3H, *p-Me*Ph). IR (cm^{-1}): 1649 (s), 1613 (m), 1593 (m), 1567 (m), 1542 (s), 1504 (s), 1463 (s), 1437 (s), 1424 (m), 1377 (s), 1351 (m), 1318 (s), 1302 (s), 1256 (m), 1200 (m), 1188 (m), 1153 (m), 1102 (w), 1055 (w), 1000 (m), 901 (w), 873 (m), 841 (s), 790 (m), 767 (s), 755 (s), 728 (s), 659(s), 632 (m), 565 (w), 517 (w), 491 (w), 462 (w), 409 (w). **1b**: Mp: 105−108 °C. ^{1}H NMR (C$_6$D$_6$, 300 MHz): δ 8.35 (d, 1H, $^3J_{H-H}$ = 3.2 Hz), 7.93 and 7.21 (AB d, 4H, ^{t}Bu−*Ph,* $^3J_{H-H}$ = 3.9 Hz), 7.59 (br s, 1H, N*H*), 6.98 (t, 1H, $^3J_{H-H}$ = 3.6 Hz), 6.64 (d, 1H, *3*-py*H*, $^3J_{H-H}$ = 8.0 Hz), 6.58 (m, 1H), 3.87 (q, 2H, C*H*$_2$, $^3J_{H-H}$ = 3.9 Hz), 2.85 (t, 2H, C*H*$_2$, $^3J_{H-H}$ = 3.9 Hz), 1.14 (s, 9H, *p-^{t}Bu*Ph). IR (cm^{-1}): 1629 (s), 1588 (w), 1542 (s), 1501 (m), 1377 (m), 1322 (m), 1271 (m), 1152 (m), 1107 (w), 1050 (w), 991 (w), 852 (w), 772 (w), 750 (w), 722 (w).

2-Py-(CH$_2$)$_2$NHC(*p-R*Ph)N*R′* (R = Me, R′ = Ph (2a); R = ^{t}Bu, R′ = 3,5-Dimethylphenyl (2b)). For **2b**: HCl (86 mL of a 1.85 M ether solution, 160 mmol) was added to a dichloromethane solution of **1b** (30.8 g, 110 mmol) and left to stir at room temperature for 45 min. PCl$_5$ (27.3 g, 131 mmol) was added to the solution followed by 3,5-dimethylaniline (40.8 mL, 327 mmol), which turned the yellow solution red upon contact. After 30 min, the slurry was heated to reflux and stirring was continued overnight. The dark red solution was cooled to room temperature and filtered away from a yellow precipitate. The solvent was removed and the resulting red solid triturated with an aqueous solution of 2 M KOH until the pH had reached ∼12. The solid was extracted into ether and washed with 2 M KOH (3 × 150 mL), brine (3 × 150 mL), and 2 M KOH (3 × 150 mL). The ether layer was dried over magnesium sulfate and the solvent concentrated to form pale yellow crystals. Further product was obtained by cooling the solution to −30 °C overnight (26 g, 63%). **2a** was prepared analogously (52%). **2a**: Mp: 121−124 °C. ^{1}H NMR (C$_6$D$_6$, 300 MHz): δ 8.51 (d, 1H, *6*-py*H*, $^3J_{H-H}$ = 4.4 Hz), 7.09 (m, 2H), 6.97 (m, 4H), 6.80 (t, 1H, *5*-py*H*, $^3J_{H-H}$ = 7.2 Hz), 6.74 (m, 4H), 6.55 (t, 1H, *4*-py*H*, $^3J_{H-H}$ = 7.2 Hz), 5.41 (br s, 1H, N*H*), 3.99 (br q, 2H, C*H*$_2$), 2.98 (br t, 2H, C*H*$_2$), 1.99 (s, 3H, *p-Me*Ph). IR (cm^{-1}): 3274 (m), 1621 (s), 1590 (m), 1541 (s), 1335 (s), 1330 (m), 1300 (m), 1142 (m), 824 (w), 722 (w). Anal. Calcd for C$_{21}$H$_{21}$N$_3$: C, 80.22; H, 6.41; N, 13.36. Found: C, 79.98; H, 6.76; N, 13.16. **2b**: Mp: 113−115 °C. ^{1}H NMR (C$_6$D$_6$, 300 MHz): δ 8.31 (d, 1H, *6*-py*H*, $^3J_{H-H}$ = 3.9 Hz), 7.29 (br d, 1H, *3*-py*H*), 7.00 (m, 3H), 6.72 (m, 2H), 6.68 (s, 2H, *o*-3,5-dimethylphenyl*H*), 6.55 (t, 1H, *4*-py*H*, $^3J_{H-H}$ = 3.9 Hz), 6.48 (s, 1H, *p*-3,5-dimethylphenyl*H*), 5.38 (br s, 1H, N*H*), 4.03 (br q, 2H, C*H*$_2$), 3.04 (br t, 2H, C*H*$_2$), 2.09 (s, 6H, 3,5-*Me*$_2$Ph), 1.04 (s, 9H, *p-^{t}Bu*-Ph). IR (cm^{-1}): 3249 (w), 1611 (s), 1590 (s), 1526 (s), 1463 (s), 1377 (m), 1317 (m), 1297 (w), 1134 (w), 994 (w), 880 (w), 837 (m), 765 (w), 701 (w). Anal. Calcd for C$_{26}$H$_{31}$N$_3$: C, 81.00; H, 8.10; N, 10.90. Found: C, 80.75; H, 8.02; N, 10.96.

[2-Py-(CH$_2$)$_2$NC(*p-R*Ph)N*R′*]$_2$Mg (R = Me, R′ = Ph (3a); R = ^{t}Bu, R′ = 3,5-Dimethylphenyl (3b)). For **3b**: To a THF solution of **2b** (4.95 g, 12.8 mmol) was slowly added Bu$_2$Mg (6.7 mL of a 0.965 M heptane solution, 6.5 mmol) via syringe, generating an orange solution. After stirring overnight, the solvent was removed in vacuo and the resulting yellow powder extracted with hexanes. Yellow crystals of **3b**(hexanes)$_{0.5}$ were obtained upon cooling to −30 °C overnight (4.61 g, 91% yield). **3a**(THF) was synthesized similarly and crystallized directly from the reaction solvent (74% yield). **3a**: Mp: 200−202 °C. ^{1}H NMR (C$_6$D$_6$, 300 MHz): δ 8.57 (d, 2H, *6*-py*H*, $^3J_{H-H}$ = 4.0 Hz), 7.27 and 6.87 (AB d, 8H, Me-*Ph*, $^3J_{H-H}$ = 7.8 Hz), 7.14−7.08 (m, 6H), 6.79 (m, 6H), 6.37−6.39 (m, 4H), 3.78 (br t, 4H, C*H*$_2$), 3.57 (br t, 8H, OC*H*$_2$CH$_2$), 2.89 (br t, 4H, C*H*$_2$), 1.99 (s, 6H, *p-Me*Ph), 1.41 (br t, 8H, OCH$_2$C*H*$_2$). IR (cm^{-1}): 1614 (m), 1584 (m), 1534 (m), 1295 (w), 1254 (w), 1144 (w), 1132 (w), 818 (w), 759 (w), 716 (m). Anal. Calcd for C$_{46}$H$_{48}$MgN$_6$O: C, 76.18; H, 6.67; N, 11.59. Found: C, 73.29; H, 6.34; N, 12.02. **3b**: Mp: 185−188 °C. ^{1}H NMR (C$_6$D$_6$, 300 MHz): δ 8.70 (d,

2H, *6*-py*H*, $^3J_{H-H}$ = 4.0 Hz), 7.30 and 7.15 (AB d, 8H, $^3J_{H-H}$ = 8.2 Hz, ^{t}Bu-*Ph*), 6.80 (s, 4H, *o*-3,5-dimethylphenyl*H*), 6.77 (t, 2H, *5*-py*H*, $^3J_{H-H}$ = 5.7 Hz), 6.44 (s, 2H, *p*-3,5-dimethylphenyl*H*), 6.35 (m, 4H), 3.84 (t, 4H, C*H*$_2$, $^3J_{H-H}$ = 6.3 Hz), 2.97 (t, 4H, C*H*$_2$, $^3J_{H-H}$ = 6.3 Hz), 2.20 (s, 12H, 3,5-*Me*$_2$Ph), 1.13 (s, 18H, *p-^{t}Bu*-Ph). IR (cm^{-1}): 1611 (s), 1590 (s), 1526 (s), 1463 (s), 1377 (m), 1317 (m), 1297 (w), 1134 (w), 994 (w), 880 (w), 837 (m), 765 (w), 701 (w). Anal. Calcd for C$_{55}$H$_{67}$N$_6$Mg: C, 78.97; H, 8.07; N, 10.05. Found: C, 78.78; H, 8.50; N, 9.79.

[2-Py-(CH$_2$)$_2$NC(*p-^{t}Bu*Ph)N(3,5-Me$_2$C$_6$H$_3$]AlMe$_2$ (4). To a −78 °C solution of **3b** (500 mg, 1.30 mmol) in ether (20 mL) was added AlMe$_3$ (1.55 mL of a 0.86 M hexane solution, 1.30 mmol) slowly via syringe. The reaction mixture was left to warm to room temperature with stirring. The solvent was removed under vacuum and the yellow solid dissolved in CH$_2$Cl$_2$. Layering with an equal volume of THF afforded yellow crystals of **4** (460 mg, 80% yield). Mp: 225 °C (dec). ^{1}H NMR (C$_6$D$_6$, 300 MHz): δ 8.61 (d, 1H, *6*-py*H*, $^3J_{H-H}$ = 3.3 Hz), 7.29 and 7.14 (AB d, 4H, $^3J_{H-H}$ = 5.1 Hz, ^{t}Bu-*Ph*), 6.83 (s, 2H, *o*-3,5-dimethylphenyl*H*), 6.77 (t, 1H, 5-py*H*, $^3J_{H-H}$ = 4.2 Hz), 6.50 (s, 1H, *p*-3,5-dimethylphenyl*H*), 6.43 (t, 1H, 4-py*H*, $^3J_{H-H}$ = 4.2 Hz), 6.29 (d, 1H, 3-py*H*, $^3J_{H-H}$ = 4.2 Hz), 3.35 (t, 2H, C*H*$_2$, $^3J_{H-H}$ = 3.6 Hz), 2.49 (t, 2H, C*H*$_2$, $^3J_{H-H}$ = 3.6 Hz), 2.09 (s, 6H, 3,5-*Me*$_2$Ph), 1.13 (s, 9H, *p-^{t}Bu*-Ph), 0.08 (s, 6H, Al*Me*$_2$). IR (cm^{-1}): 1608 (m), 1597 (m), 1570 (m), 1477 (s), 1450 (s), 1424 (sh), 1360 (m), 1340 (m), 1260 (w), 1179 (w), 1167 (w), 1159 (w), 1135 (w), 1120 (w), 1103 (w), 1021 (m), 850 (m), 799 (w), 767 (m), 755 (m), 709 (m), 692 (m), 665 (m). Anal. Calcd. for C$_{28}$H$_{36}$N$_3$Al: C, 76.16; H, 8.22; N, 9.52. Found: C, 75.85; H, 8.59; N, 9.51.

[2-Py-(CH$_2$)$_2$NC(*p-^{t}Bu*Ph)N(3,5-Me$_2$C$_6$H$_3$]Zr(CH$_2$Ph)$_3$ (5). A diethyl ether solution (100 mL) of Zr(CH$_2$Ph)$_4$ (5.00 g, 10.5 mmol) was added via cannula to a solution of **2b** (4.07 g, 10.5 mmol) in Et$_2$O (750 mL) to generate a red solution and a yellow precipitate. After stirring at room-temperature overnight, the mixture was filtered and the resultant yellow powder dried in vacuo. Concentration of the filtrate and cooling to −30 °C induced further crystallization (yield 5.75 g, 75%). Mp: 165 °C (dec). ^{1}H NMR (C$_6$D$_6$, 300 MHz): δ 8.69 (d, 1H, *6*-py*H*, $^3J_{H-H}$ = 4.2 Hz), 7.22−7.10 (m, 15H), 6.96−6.88 (m, 6H), 6.70 (t, 1H, *5*-py*H*, $^3J_{H-H}$ = 6.0 Hz), 6.56 (s, 1H, *p*-3,5-dimethylphenyl*H*), 6.30 (t, 1H, *4*-py*H*, $^3J_{H-H}$ = 6.0 Hz), 6.15 (d, 1H, *3*-py*H*, $^3J_{H-H}$ = 7.8 Hz), 2.90 (s, 6H, C*H*$_2$Ph), 2.43 (t, 2H, C*H*$_2$, $^3J_{H-H}$ = 5.7 Hz), 2.12 (s, 6H, 3,5-*Me*$_2$Ph), 1.52 (t, 2H, C*H*$_2$, $^3J_{H-H}$ = 5.7 Hz), 1.07 (s, 9H, *p-^{t}Bu*-Ph). IR (cm^{-1}): 1606 (m), 1590 (s), 1565 (w), 1423 (m), 1376 (w), 1345 (m), 1314 (m), 1205 (s), 1118 (m), 1023 (m), 964 (s), 951 (m), 917 (s), 885 (w), 849 (w), 836 (m), 793 (m), 743 (s), 697 (s), 629 (w), 539 (w), 516 (w). Anal. Calcd for C$_{47}$H$_{51}$N$_3$Zr: C, 75.35; H, 6.86; N, 5.61. Found: C, 72.39; H, 6.41; N, 5.65.

[2-Py-(CH$_2$)$_2$NC(*p-Me*Ph)NPh]$_2$La[N(SiMe$_3$)$_2$] (6). 2a (1.00 g, 3.18 mmol) in ether (30 mL) was added dropwise via cannula to an ethereal solution (20 mL) of La[N(SiMe$_3$)$_2$]$_3$ (983 mg, 1.59 mmol) maintained at −78 °C. The solution was left to warm to room temperature with stirring. The volume was reduced and the reaction solution layered with hexanes. Upon standing overnight, pale yellow crystals of **6** formed (603 mg, 42% yield). Mp: 220 °C (dec). ^{1}H NMR (C$_6$D$_6$, 300 MHz): δ 9.61 (d, 2H, *6*-py*H*, $^3J_{H-H}$ = 4.2 Hz), 7.07 and 6.66 (AB d, 8H, $^3J_{H-H}$ = 7.8 Hz, Me−*Ph*), 6.76 (m, x*H*), 6.50 (t, 2H, 3-py*H*, $^3J_{H-H}$ = 7.2 Hz), 6.30 (d, 2H, 2-py*H*, $^3J_{H-H}$ = 7.2 Hz), 3.27 (br s, 4H, C*H*$_2$), 2.95 (br s, 4H, C*H*$_2$), 1.88 (s, 6H, *p-Me*Ph), 0.60 (s, 18H, N(Si*Me*$_3$)$_2$). IR (cm^{-1}): 1600 (m), 1591 (m), 1566 (m), 1347 (m), 1327 (m), 1314 (m), 1261 (m), 1236 (m), 1179 (w), 1152 (w), 1103 (w), 988 (s), 870 (m), 824 (s), 768 (w), 735 (w), 695 (w), 662 (w), 597 (w). Anal. Calcd for C$_{48}$H$_{58}$LaN$_7$Si$_2$: C, 62.12; H, 6.30; N, 10.56. Found: C, 60.08; H, 5.86; N, 10.16.

General Procedures for X-ray Crystallography. Pertinent details for the individual compounds can be found in Table 6. A crystal of appropriate size was mounted on a glass capillary using Paratone-N hydrocarbon oil. The crystal was

transferred to a Siemens SMART diffractometer/CCD area detector,[27] centered in the beam, and cooled by a nitrogen flow low-temperature apparatus which had been previously calibrated by a thermocouple placed at the same position as the crystal. Preliminary orientation matrix and cell constants were determined by collection of 60 10-s frames, followed by spot integration and least-squares refinement. A hemisphere of data was collected, and the raw data were then integrated (XY spot spread = 1.60°; Z spot spread = 0.60°) using SAINT.[28] Cell dimensions reported in Table 6 were calculated from all reflections with $I > 10\sigma$. Data analysis and absorption correction were performed using Siemens XPREP[29] and SADABS. The data were corrected for Lorentz and polarization effects, but no correction for crystal decay was applied. The reflections measured were averaged. The structures were solved and refined with the teXsan software package[30] using direct methods[31] and expanded using Fourier techniques. All non-

hydrogen atoms were refined anisotropically, unless stated otherwise. Hydrogen atoms were assigned idealized positions and were included in structure factor calculations, but were not refined, unless stated otherwise. The final residuals were refined against the data for which $F^2 > 3\sigma(F^2)$. The quantity minimized by the least-squares program was $\sum_w(|F_o| - |F_c|)^2$, where w is the weight of a given observation. The p factor, used to reduce the weight of intense reflections, was set to 0.03 throughout the refinement. The analytical forms of the scattering factor tables for the neutral atoms were used, and all scattering factors were corrected for both the real and imaginary components of anomalous dispersion.

Supporting Information Available: Tables of positional and thermal parameters and bond distances and angles for all crystallographically characterized compounds. This material is available free of charge via the Internet at http://pubs.acs.org.

OM990365W

(24) Zucchini, U.; Giannini, U.; Albizatti, E.; D'Angelo, R. *Chem. Commun.* **1969**, 1174.
(25) Zucchini, U.; Giannini, U.; Albizzati, E. *J. Organomet. Chem.* **1971**, *26*, 357.
(26) Evans, W. J.; Golden, R. E.; Ziller, J. W. *Inorg. Chem.* **1991**, *30*, 4963.
(27) *SMART* Area-Detector Software Package; Madison, WI, 1993.
(28) *SAINT*: SAX Area-Detector Integration Program; Madison, WI, 1995.
(29) *XPREP*: Part of the SHELXTL Crystal Structure Determination Package; Madison, WI, 1995.
(30) *TeXsan*: Crystal Structure Analysis Package; Molecular Structure Corporation: The Woodlands, TX, 1992.

(31) *SIR92*: Altomare, A.; Burla, M. C.; Camilli, M.; Cascarano, M.; Giacovazzo, C.; Guagliardi, A.; Polidori, G. *J. Appl. Crystallogr.* **1993**, *26*, 343.